Talanta 99 (2012) 487–491

Contents lists available at SciVerse ScienceDirect

Talanta

journal homepage: www.elsevier.com/locate/talanta

Electrochemical determination of NADH based on MPECVD carbon nanosheets

Zhipeng Wang [a,b,*], Mao Shoji [b], Hironori Ogata [a,b,**]

[a] Institute for Sustainability Research and Education, Hosei University, 2–17–1, Fujimi, Chiyoda-Ku, Tokyo 102-8160, Japan
[b] Department of Chemical Science and Technology, Faculty of Bioscience and Applied Chemistry & Graduate School of Engineering, Hosei University, 3-7-2, kajino-cho, koganei, Tokyo 184–8584, Japan

ARTICLE INFO

Article history:
Received 8 May 2012
Received in revised form
5 June 2012
Accepted 6 June 2012
Available online 18 June 2012

Keywords:
Electrochemical biosensor
Multilayer graphene
Carbon nanosheets
MPECVD
NADH

ABSTRACT

Characterization and application of carbon nanosheets (CNSs) grown by microwave plasma enhanced chemical vapor deposition (MPECVD) have been investigated for the electrochemical biosensor. The as-grown CNS films possess a porous structure with a large amount of graphene edges which most of them are less than 2 nm in thickness, as confirmed by scanning and transmission electron microscopes. "Surface-sensitive" probe, $Fe(CN)_6^{3-/4-}$, exhibits that the original CNSs have faster electron transfer than glassy carbon electrode, owing to much more edge plane sites on the original CNS surface. "Oxygen-sensitive" probe, $Fe^{3+/2+}$ also confirmed that the oxygen species in the CNS film can improve its electrochemical activity. The modified electrode by MPECVD CNS films has been used to detect NADH for the first time. The CNSs with many graphene edges efficiently catalyse the oxidation of NADH at 0.336 V. The biosensor linearly responds to NADH in the range of 0–500 μM (R=0.99665), the sensitivity of the electrode is 85.8 mA M^{-1} or 715 mA M^{-1} cm^{-2}, and the detection limit of NADH is about 0.44 μM (S/N=3). The biosensor also displays excellent stability for NADH detection and good selectivity in the interference from ascorbic acid.

1. Introduction

The determination of β-nicotinamide adenine dinucleotide (NADH) based on electrochemical sensors has attracted considerable attention because NADH is considered as a cofactor in several hundred enzymatic reactions of $NADH/NAD^+$-dependent dehydrogenases [1,2]. However, the electrochemical oxidation of NADH at a traditional solid electrode (bare Pt or glassy carbon electrode) encounters some problems, such as large overvoltage and surface fouling associated with the adsorption of reaction products [3]. Consequently, numerous efforts have been devoted to identifying new electrode materials and new methods that can reduce the overvoltage for NADH oxidation and minimize the surface fouling effect. With the rapid development of nanotechnology, the nanoscale materials, including metal and semiconductor nanoparticles [4–6], polymers [7,8], carbon nanotubes (CNTs) [9–11] and carbon nanofibers (CNFs) [12–15], have been employed successfully to solve these mentioned-above problems related to NADH oxidation. Especially, carbon-based nanomaterials, owing to their inertness, relatively wide potential window and low background current, have been extensively used in both analytical and industrial electrochemistry [9–17]. It has been shown that the carbon nanostructures have excellent electron transfer kinetics which is beneficial from special morphologies, novel electronic structures, and high electrical conductivity [18]. Currently, the hottest material in the carbon family is graphene, consisting of a single layer of sp^2-hybridized carbon atoms connected by covalent bonds to form a hexagonal atomic sheet, which has received great interest in electronic devices and biosensors because of their fascinating properties [19,20]. Considered high productivity of graphene synthesis and simple electrode preparation, current electrode systems as NADH sensors mainly focus on the reduced graphene oxides which convert graphene oxides into graphene with the nature of single sheet by chemical treatments [21–23]. However, this approach leads to more or less some residuals (acids, oxides) in graphene sheets after chemical treatments and water cleaning. Moreover, the posttreatment processes also cause the re-aggregation of graphene sheets. It must affect the electrochemical behaviors of graphene sheets as NADH sensors, and then reduces the repeatability of modified electrodes. Therefore, improving the repeatability of the electrodes is still important and significant in biosensors. In this work, we employ microwave plasma enhanced chemical vapor deposition (MPECVD) to produce the carbon nanosheets (CNSs), which can be utilized to directly modify the bare electrode as biosensors without destroying original structure for detecting NADH. Thus, CNS-modified electrode can not only rule out the effects of acids and oxides and retain its high repeatability, but also exhibit its intrinsic properties.

* Corresponding author at: Hosei University Institute for Sustainability Research and Education 2–17–1, Fujimi, Chiyoda-Ku, Tokyo 102-8160, Japan.
Tel.: +81 42 387 6172.
** Corresponding author.
E-mail addresses: wangzhipeng11@gmail.com (Z. Wang), hogata@hosei.ac.jp (H. Ogata).

0039-9140/$ - see front matter © 2012 Elsevier B.V. All rights reserved.
http://dx.doi.org/10.1016/j.talanta.2012.06.014

CNSs, one of the multilayer graphene materials, can be described as graphite sheet nanostructures with a large number of edges that are composed of stacks of planar graphene sheets standing almost vertically on the substrate [24]. Due to the exceptional properties such as high surface area, high conductivity and chemical inertness, CNSs should be ideal candidates as electrode materials [25,26]. Recently, we obtained CNS films by MPECVD technique in Ar-CH_4 system at relatively low temperatures [27]. The CNS films possess flower-like structures with a large amount of sharp edges which consist of graphene sheets with nanometer scales. Moreover, the CNS films can be easily peeled from the Cu substrate by controlling experimental parameters. Thus, the CNS films can be transferred to the surface of bare electrode by only a tweezers with the help of some ethanol, and then dried by a halogen lamp for 5–10 min to fabricate a modified electrode. Obviously, this approach is simpler than those traditional preparation methods for CNTs and graphene. It has been demonstrated that the prepared CNS-modified electrode as a biosensor exhibits an excellent electrocatalytic performance for detecting the dopamine with the present of uric acid and ascorbic acid in phosphate buffer solution [28]. It suggests that the excellent electron transfer properties involve in the interface between the CNS surface and the electrolyte due to graphene structures. Compared with CNTs and monographene that have gained considerable attention, the as-grown CNSs possess more defects on the edge sites which exhibit more excellent electrocatalytic activity. Here, we further explore the new applications of CNSs in the field of the electrochemical biosensors. To the best of our knowledge, the application of CNS films obtained by MPECVD as an electrode material for NADH oxidation is presented for the first time. This CNS-modified electrode shows an obvious decrease in the overvoltage of NADH oxidation and a relatively low detection limit of NADH in buffer solution.

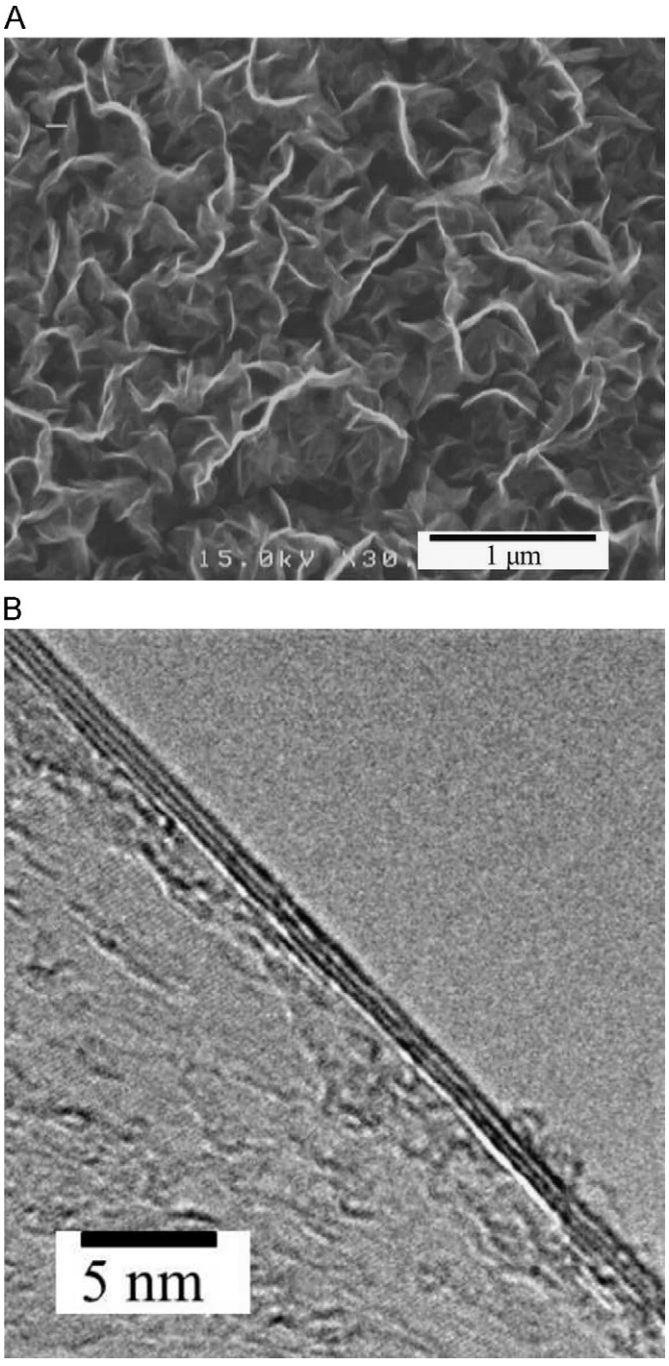

Fig. 1. (A) SEM and (B) TEM images of the CNS films grown on the Cu surface by MPECVD.

2. Materials and methods

β-Diphosphopyridine nucleotide disodium salt (reduced form, NADH), potassium hexacyanoferrate (III), ammonium iron (III) sulfate 12-water, sodium dihydrogenphosphate dihydrate, perchloric acid and sodium hydroxide were purchased from Wako,

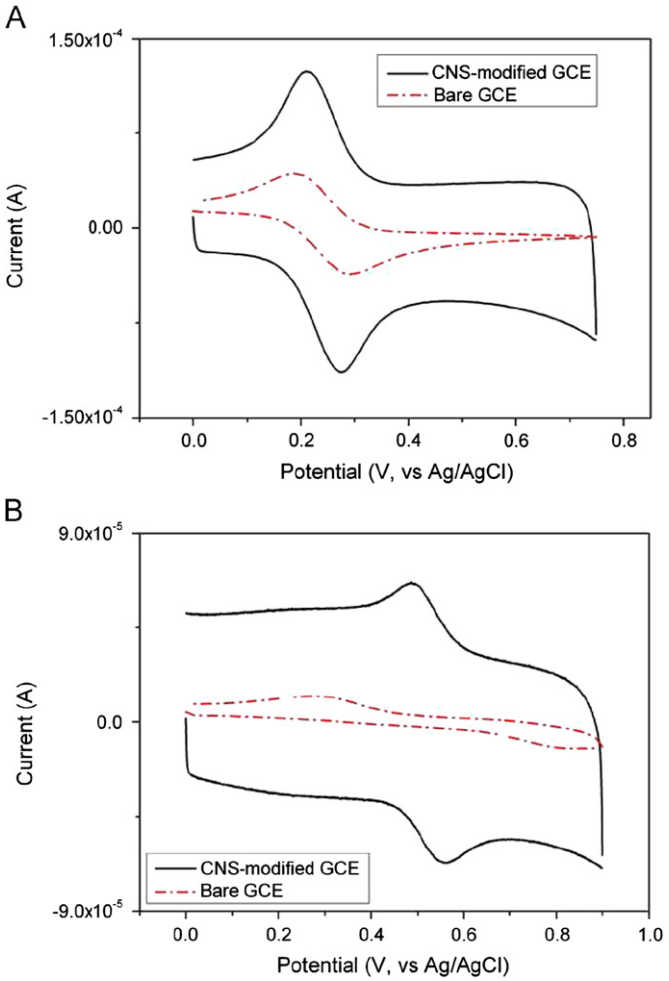

Fig. 2. CV responses obtained for bare (dash dot line) and the CNS-modified (solid line) GCEs in (A) 5 mM $Fe(CN)_6^{3-}$ with 1 M KCl. (B) 3 mM Fe^{3+} with 0.2 M $HClO_4$ Scan rate: 200 mV s^{-1}.

pure chemical industries, Ltd. Potassium chloride was obtained from NACALAI TESQUE, INC. Cu foil was provide by Nilaco. All gases including N_2, CH_4, Ar were bought from Iwatani. All solutions were prepared with deionized water.

CNS was prepared by MPECVD with the gas sources of Ar and CH_4 at the temperature less than 500 °C. The detailed growth conditions can be found in our previous papers [27,29]. Prior to modification, the glassy carbon electrode (GCE, Ø=3 mm) was polished with 0.05 μm alumina slurry and then washed by deionized water. Sequentially, the clean GCE with some ethanol was covered by CNS films (3 mm × 4 mm × 10 μm) using a tweezers. Finally, the CNS-modified GCE was dried by a halogen lamp for 5–10 min.

The morphology and microstructure of CNS films were investigated by scanning (SEM, S-4500, Hitachi) and transmission (TEM, JEM-2100F, JEOL) electron microscopies, respectively. All electrochemical measurements were conducted with a CHI 600C electrochemical workstation assembled with a three-electrode system using a GCE or modified GCE as working electrode, a Pt wire as counter electrode, and a Ag/AgCl (3 M KCl) electrode as reference electrode. All potentials were reported in this context with respect to this reference. Before the electrochemical experiments, all solution to be measured was purged with nitrogen gas for about 10 min. The electrodes were kept in the air at room temperature when not in use.

3. Results and discussion

3.1. Characteristization of CNS films

We first characterized the morphology and microstructure of as-synthesized CNS films. Fig. 1A and B show typical SEM and TEM images of the CNS grown on the Cu substrate, respectively. It can be found that the CNS films have a porous structure, and consist of a large amount of defects on the graphene edges which most of them is less than 2 nm in thickness.

3.2. Electrochemical characteristics of CNS films

The CNSs synthesized have a large amount of graphitic shape edges which provide an ideal system as an electrode material in electrochemical sensing and biosensing. Due to be sensitive to the nature of surface, the redox system of $Fe(CN)_6^{3-/4-}$ was used to probe the CNSs firstly [30]. Fig. 2A shows a typical comparison of cyclic voltammograms (CVs) between bare and modified GCEs in 1 M KCl containing 5 mM $Fe(CN)_6^{3-}$ at the scan rate of 200 mV s^{-1}. It can be seen that peak current at modified electrode increased due to the large electrochemically active surface area of the CNSs. Two well-defined redox peaks with the potential separations (ΔE_p) of 93 and 64 mV were observed for bare and modified GCEs, respectively. The small value of peak to peak separation for CNS-modified electrode may be partly due to the thin-layer effect that was caused by the nature of the porosity of the CNS films [31,32]. However, it can be confirmed that the reaction of $Fe(CN)_6^{3-/4-}$ on the CNS surface was dominated by the diffusion process according to the linear relation between the current response and square root of the voltage scan rate. Thus, it means that the CNS-modifed GCE can cause a significant increase in the electron transfer rate to $Fe(CN)_6^{3-/4-}$. It is attributed to the high proportion of edge plane sites and defects present in the graphene nanosheets, due to their small lateral size. It is compatible to reports by McCreery group, whose experiments exhibited the electron transfer rate of $Fe(CN)_6^{3-/4-}$ for glassy carbon faster than that for highly ordered pyrolytic graphite (HOPG) because of glassy carbon having many exposed graphitic edges [30].

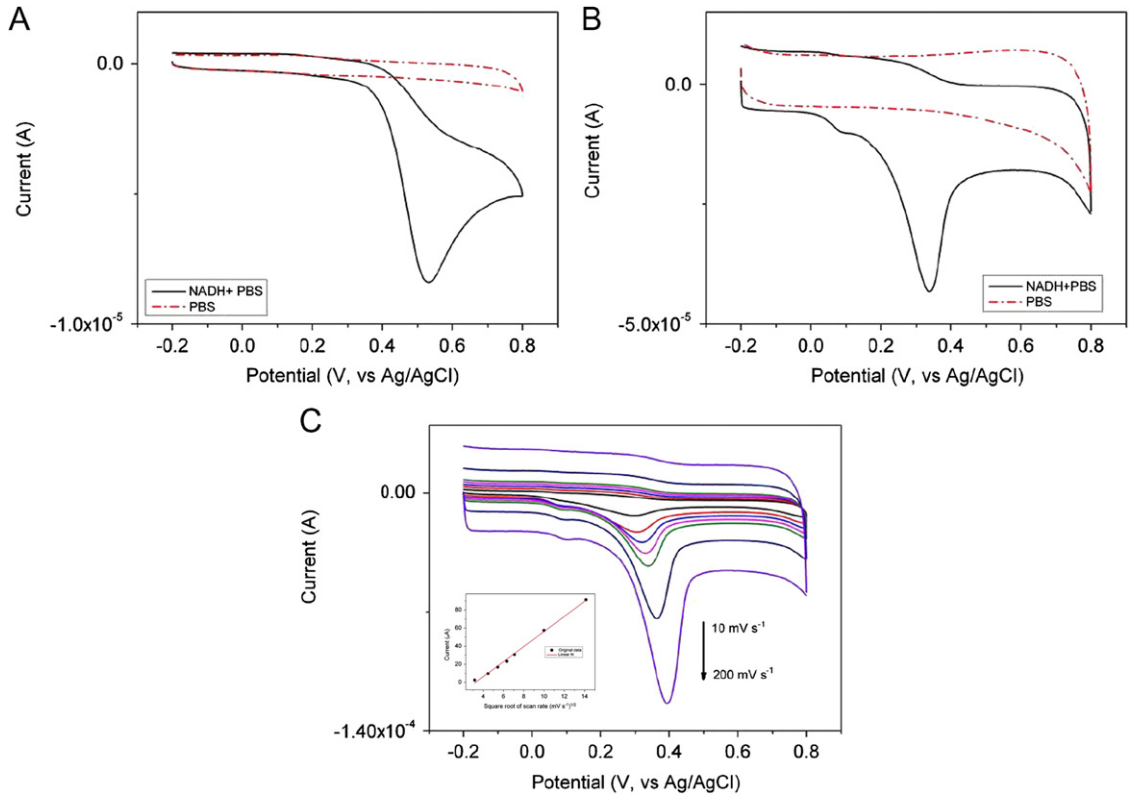

Fig. 3. CV responses obtained in 0.1 M pH 7.0 PBS with the absence (dash dot line) and presence (solid line) of 1 mM NADH at (A) bare and (B) the CNS-modified GCEs. Scan rate: 50 mV s^{-1}. (C) CV responses at the CNS-modified GCE in 0.1 M pH 7.0 PBS containing 1 mM NADH at the different scan rates from 10 to 200 mV s^{-1}. Inset shows the relationship between the peak current and the square root of scan rate.

Besides the edge plane sites/defects, oxygen-rich species present on the carbon surface also could be responsible for NADH oxidation at lower overvoltages. As reported previously, $Fe(CN)_6^{3-/4-}$ is "surface-sensitive" but not "oxide-sensitive", while $Fe^{3+/2+}$ probe depends strongly on surface oxide level [30]. In the following, the CNS-modified electrodes were measured by cycling in 0.2 M $HClO_4$ solution containing 3 mM Fe^{3+} between 0 and +0.9 V at the scan rate of 200 mV s^{-1}. Fig. 2B shows that GCE exhibit an extremely sluggish response to this probe, whereas the CNS electrode gives rise to well-defined CV response, indicative of rapid electron transfer. It indicates that $Fe^{3+/2+}$ electron transfer was accelerated by some oxygen groups in the CNSs, which was confirmed previously by X-ray photoelectron spectroscopy [27].

3.3. Electrocataytic oxidation of NADH on CNS-modified electrode

The fast and reliable detection of NADH at low potential are especially significant. The CV responses at bare and the CNS-modified GCEs obtained in 0.1 M phosphate buffer solution (PBS) of pH 7.0 in the absence and presence of 1 mM NADH are shown in Fig. 3. As shown in Fig. 3A, an oxidation peak at +0.530 V appeared at a bare GCE in the presence of NADH in PBS, compared to the oxidation curve without an obvious peak in the absence of NADH. This response is in accordance with other literatures [10,23]. It is worth noting that bare GCE is highly susceptible to electrode passivation from the strong adsorption of the oxidized form, NAD^+, of NADH so that the oxidation potential is easily shifted to high level. At the CNS-modified GCE, no visible voltammetric response was yet observed in PBS without NADH, as shown in Fig. 3B. This can rule out the effects of quinines which were usually formed on the surface of CNTs or CNFs treated by acids.[6,7] Nevertheless, upon the addition of 1 mM NADH to PBS, two anodic peaks with different shapes and intensities were appeared at +0.082 and +0.336 V in the curve. The anodic peak potentials are very similar to those obtained for the treated CNF which showed two oxidation peaks at +0.062 and +0.361 V (both *vs* SCE) in 0.2 M pH 7.0 PBS with 2.0 mM NADH at a sweep rate of 10 mV s^{-1}[12]. The authors explained that two wave responses could be ascribed to NADH oxidation at the edge plane sites on the CNF and those of the underlying GCE, which these based on Compton' analyses about CNTs. However, note that the positions of potentials are different from those for CNT-modified electrodes at +0.270 and +0.430 V [10], and +0.330 and +0.570 V [9] (all *vs* Ag/AgCl, 50 mV s^{-1}). In addition, the relative intensities of two peaks are different for the CNT-modified electrodes and our samples. It means that there exist other reasons which are responsible for the current results. Although we have not yet known the exact reason for the different characteristic peaks at present, we think that it may be ascribed to the special porous structure of CNSs. Whatever, it is undoubted that these anodic peaks can be attributed to electrocatalytic oxidation of NADH at the CNS-modified electrode. In contrast to bare GCE, the anodic peak potential is negatively shifted when the GCE is modified by the CNS films. Compared to that obtained for bare GCE at +0.530 V, the peak current density at the modified at +0.336 V also increased from 110.6 to 255.1 μA cm^{-2}. These results indicate that the CNS films can promote the electron transfer between NADH and electrode due to graphene-related structures, edge plane defects, and oxygen-rich groups on the CNS surface. Fig.3C shows CV responses of the CNS-modified GCE in 0.1 M PBS containing 1 mM NADH at the different scan rates from 10 to 200 mV s^{-1}. It can be found that the oxidation potential increase with increasing scan rates toward a more positive potential, indicating the electrochemical irreversibility of the electrochemical reaction. The relationship between the peak currents and square root of scan rates was plotted linearly, suggesting that the transfer process between the CNS surface and electrolyte is controlled by diffusion, which is similar to graphene-modified GCEs [10,17,23].

Next, we investigate the sensing possibility of the CNS-modified GCE by using linear scan voltammogram (LSV). Fig. 4A shows LSV responses of the CNS-modified GCE in 0.1 M pH 7.0 PBS with various NADH concentrations from 0 to 500 μM at the scan rate of 50 mV s^{-1}. The inset in Fig. 4A is the enlarged pattern of low NADH contents in the range of 0–20 μM. The electrochemical oxidation currents of NADH increase with respect to their increasing concentrations, and the peak potential was slightly shifted to more positive potential as the concentration of NADH was increased. The positively slight shift of the potential is probably incited by NAD^+ produced at the elevated NADH concentrations, as observed by others [33–35]. The corresponding relationship between the current intensity and NADH concentration is shown in Fig. 4B. It can be observed that they have the linear relation with a linear regression equation of $I_{pa}(A)=8.5834E\text{-}8*C_{NADH}$ (μM)+8.548E-8 with $R=0.99665$ over NADH concentration range of 0–500 μM. The sensitivity was found to be 85.8 mA M^{-1} or 715 mA M^{-1} cm^{-2} in term of geometry area. The value is much larger than most of values for NADH biosensors previously reported based on carbon nanomaterials. According to the definition, it is estimated that the detection limit of NADH is about 0.44 μM (S/N=3), which is lower than those at graphene-based sensors [23,36].

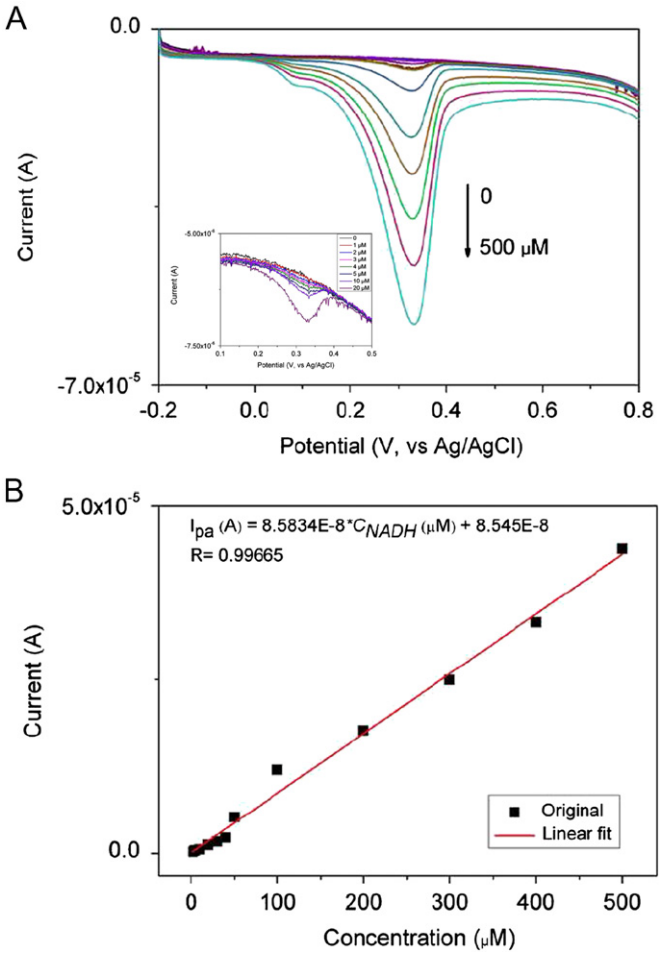

Fig. 4. (A) LSV responses obtained at the CNS-modified (solid line) GCE in 0.1 M pH 7.0 PBS with different NADH concentrations from 0 to 500 μM with the scan rate of 50 mV s^{-1}. Inset shows an enlarged pattern at low NADH concentrations. (B) Peak current *vs* NADH concentration. Inset shows the corresponding linear regression and *R*.

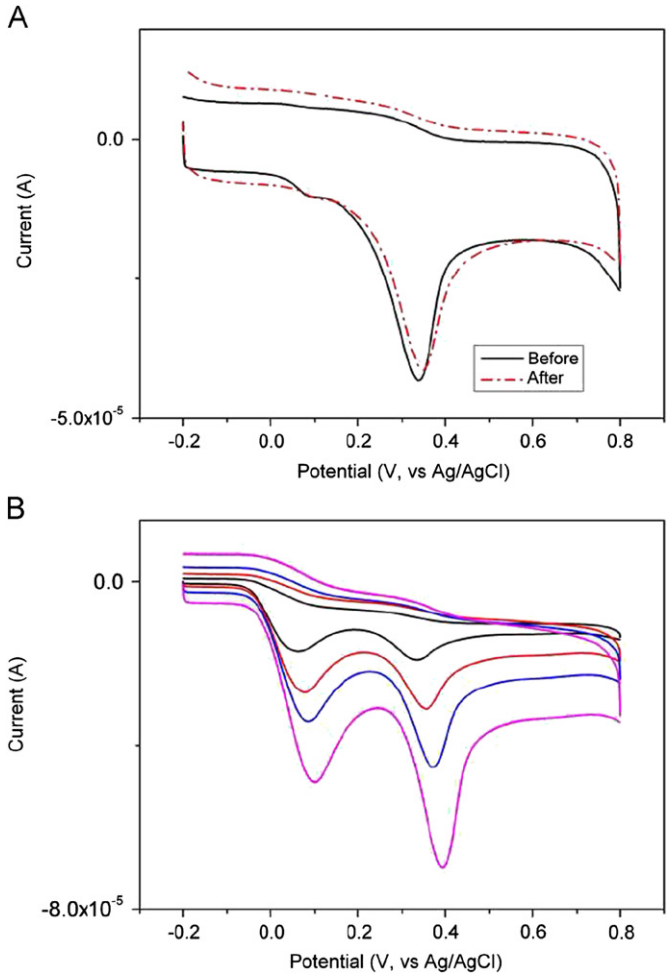

Fig. 5. (A) CV responses obtained in 0.1 M pH 7.0 PBS containing 1 mM NADH at the CNS-modified GCE that was used before (solid line) and after (dash dot line) being kept for a week at room temperature. (B) CV responses of the CNS-modified Pt electrode in in 0.1 M pH 7.0 PBS containing 1 mM NADH and 1 mM AA. Scan rates: 20, 50, 100, and 200 mV s^{-1}.

3.4. Stability and selectivity of CNS-modified electrode

The stability of biosensor for detecting NADH is also an important feature. Before employed for exploring stability, the electrode has been used for all experiments in Figs. 2 and 3, and then kept in the air at room temperature without any protection. Fig. 5A shows the comparison of the CNS-modified GCE before and after being kept for one week without special treatment. It can be seen that the oxidation response of NADH displays a positive shift of 12 mV with a little decrease in the peak current and a slight increase in background current after cycling the electrode again. The result implies that the stability of the CNS-modified electrode is very excellent, and it is suitable for the determination of NADH.

Selective detection of NADH is very important in the development of NADH biosensor. Ascorbic acid (AA) is a common interference in the electrochemical determination of biological substances such as NADH because AA exhibits similar electrochemical response at a conventional electrode. Fig. 5B shows CV responses of the CNS electrode in 0.1 M pH 7.0 PBS containing 1 mM AA and 1 mM NADH with various scan rates. The new electrode was prepared by the CNS films (2 mm × 3 mm × 10 μm) modified Pt disc electrode (Ø=1.6 mm) with same procedure as mentioned above. At the scan rate of 50 mV s^{-1}, the peak at +0.078 V is attributed to the electrochemical oxidation of AA with NADH oxidation peak at +0.355 V. The separation of 267 mV is obtained, suggesting that the selective determination of NADH in the presence of AA is feasible at the CNS-modified electrode.

4. Conclusions

In summary, the CNSs grown by MPECVD technique have been firstly employed to determine NADH. The CNS-modified electrodes possess not only high repeatability because of simple preparation procedure, but also demonstrate a substantial decrease in the overvoltage of NADH oxidation with high sensitivity, selectivity as well as stability due to a large amount of edge plane sites/defects and oxygen-rich group on the CNS surface. Thus, the MPECVD-synthesized CNSs have bright and broad prospects in the application of electrochemical biosensors.

Acknowledgement

The authors appreciate Mr Masaki Ichihara of Hosei University for the technical support of TEM.

References

[1] A. Bergel, J. Souppe, M. Comtat, Anal. Biochem. 179 (1989) 382–388.
[2] A. Radoi, D. Compagnone, Bioelectrochemistry 76 (2009) 126–134.
[3] B.A. Deore, M.S. Freund, Chem. Mater. 17 (2005) 2918–2923.
[4] B. Shlyahovsky, E. Katz, Y. Xiao, V. Pavlov, I. Willner, Small 1 (2005) 213–216.
[5] J. Huang, D. Wang, H. Hou, T. You, Adv. Funct. Mater. 18 (2008) 441–448.
[6] L. Bahshi, R. Freeman, R. Gill, I. Willner, Small 5 (2009) 676–680.
[7] F. Valentini, A. Salis, A. Curulli, G. Palleschi, Anal. Chem. 76 (2004) 3244–3248.
[8] S.A. Kumar, S.-M. Chen, Sensors 8 (2008) 739–766.
[9] M. Musamen, J. Wang, A. Merkoci, Y. Lin, Electrochem. Commun. 4 (2002) 743–746.
[10] C.E. Banks, R.G. Compton, Analyst 130 (2005) 1232–1239.
[11] Q. Wang, H. Tang, Q. Xie, L. Tan, Y. Zhang, B. Li, S. Yao, Electrochim. Acta 52 (2007) 6630–6637.
[12] L. Wu, X. Zhang, H. Ju, Anal. Chem. 79 (2007) 453–458.
[13] A. Arvinte, F. Valentini, A. Radoi, F. Arduini, E. Tamburri, L. Rotariu, G. Palleschi, C. Bala, Electroanal. 19 (2007) 1455–1459.
[14] Y. Liu, H. Hou, T. You, Electroanal. 20 (2008) 1708–1713.
[15] M.L. Weeks, T. Rahman, P.D. Frymier, S.K. Islam, T.E. McKnight, Sens. Actuator B 133 (2008) 53–59.
[16] Y. Zhou, J. Zhi, Talanta 79 (2009) 1189–1196.
[17] F. Gao, X. Guo, J. Yin, D. Zhao, M. Li, L. Wang, RAC Adv 1 (2011) 1301–1309.
[18] J. Wang, Electroanal. 17 (2005) 7–14.
[19] M. Pumera, Chem. Soc. Rev. 39 (2010) 4146–4157.
[20] Y. Shao, J. Wang, H. Wu, J. Liu, I.A. Aksay, Y. Lin, Electroanal. 22 (2010) 1027–1036.
[21] C. Shan, H. Yang, D. Han, Q. Zhang, A. Ivaska, L. Niu, Biosens. Bioelectron. 25 (2010) 1504–1508.
[22] T. Kuila, S. Bose, P. Khanra, A.K. Mishra, N.H. Kim, J.H. Lee, Biosens. Bioelectron. 26 (2011) 4637–4648.
[23] S.P. Kumar, R. Manjunatha, C. Nethravathi, G.S. Suresh, M. Rajamathi, T.V. Venkatesha, Electroanal. 23 (2011) 842–849.
[24] M. Hiramatsu., M. Hori, Carbon Nanowalls, SpringerWien, New York, 2010.
[25] E. Luais, M. Boujtita, A. Gohier, A. Tailleur, S. Casimirius, M.A. Djouadi, A. Granier, P.Y. Tessier, Appl. Phys. Lett. 95 (2009) 014104.
[26] X. Zhao, H. Tian, M. Zhu, K. Tian, J.J. Wang, F. Kang, R.A. Outlaw, J. Power Sources 194 (2009) 1208–1212.
[27] Z. Wang, M. Shoji, H. Ogata, Appl. Surf. Sci. 257 (2011) 9082–9085.
[28] Z. Wang, M. Shoji, H. Ogata, Analyst 136 (2011) 4903–4905.
[29] Z. Wang, M. Shoji, H. Ogata, Jpn. J. Appl. Phys. 51 (2012) 01AH02.
[30] R.L. McCreery, Chem. Rev. 108 (2008) 2646–2687.
[31] I. Streeter, G.G. Wildgoose, L. Shao, R.G. Compton, Sens. Actuator B 133 (2008) 462–466.
[32] M.C. Henstridge, E.J.F. Dickinson, M. Aslanoglu, C. Batchelor-McAuley, R.G. Compton, Sens. Actuator B 145 (2010) 417–427.
[33] C. Retna Raj, T. Ohsaka, Bioelectrochemistry 53 (2001) 251–256.
[34] B.K. Jena, C.Retna Raj, Anal. Chem. 78 (2006) 6332–6339.
[35] K.M. Manesh, P. Santhosh, A. Gopalan, K.P. Lee, Talanta 75 (2008) 1304–1307.
[36] M. Zhou, Y. Zhai, S. Dong, Anal. Chem. 81 (2009) 5603–5613.